Quantum theory of cold bosonic atoms in optical lattices

Dagim Tilahun,[1,2] R. A. Duine,[3] and A. H. MacDonald[1]
[1]*Department of Physics, The University of Texas at Austin, Austin, Texas 78712, USA*
[2]*Department of Physics, Texas State University, San Marcos, Texas 78666, USA*
[3]*Institute for Theoretical Physics, Utrecht University, Leuvenlaan 4, NL-3584 CE Utrecht, The Netherlands*
(Received 15 May 2011; published 16 September 2011)

Ultracold atoms in optical lattices undergo a quantum phase transition from a superfluid to a Mott insulator as the lattice potential depth is increased. We describe an approximate theory of interacting bosons in optical lattices which provides a qualitative description of both superfluid and insulator states. The theory is based on a change of variables in which the boson coherent state amplitude is replaced by an effective potential which promotes phase coherence between different number states on each lattice site. It is illustrated here by applying it to uniform and fully frustrated lattice cases but is simple enough that it can be applied to spatially inhomogeneous lattice systems.

DOI: 10.1103/PhysRevA.84.033622 PACS number(s): 67.85.−d, 64.70.Tg

I. INTRODUCTION

The observation [1] of a cold-atom quantum phase transition between superfluid (SF) and Mott insulator (MI) states was important on its own merits and because it suggested future experimental studies of clean, highly controllable, strongly correlated bosonic many-body systems. The promise of early experiments has been borne out by studies that have demonstrated unprecedented experimental control in designing and investigating many-body systems whose Hamiltonian's are known with a level of precision that is uncommon in condensed-matter physics [2]. Cold-atom systems are not, however, completely free of the real-world complications that can confuse the interpretation of experiments. The most obvious troublesome complications in simulating condensed-matter many-body physics problems using cold atoms are that experimental systems are always spatially inhomogeneous to some degree and that they are often fairly small. In most cases, the spatial inhomogeneity is an undesirable consequence of an experimental necessity, for example, the harmonic trapping potential employed in most cold-atom setups. In some cases, though, it is the central focus of the experiment, as in studies of disorder in strongly correlated bosonic systems [3,4]. In this paper we describe an approximate theory of strongly interacting bosons in an optical lattice that is sophisticated enough to achieve a good qualitative description of both Mott insulator and superfluid limits and yet simple enough that it can be applied with relative ease to finite spatially inhomogeneous bosonic optical lattice experiments. The theory is a generalization of the mean-field theory of the MI-SF phase transition in which the potential which induces coherence between different number states on a given lattice site is elevated from a variational parameter to a fluctuating quantum variable. We illustrate the potential of this simple theory by applying it to uniform optical lattice systems with constant and fully frustrated intersite hopping parameters.

The systems in which we are interested provide an approximate realization of the Bose-Hubbard Hamiltonian (BHH) [5],

$$H_{\mathrm{BHH}} = \frac{1}{2}\sum_i U n_i(n_i-1) - \sum_i(\mu-\epsilon_i)n_i - \sum_{\langle i,j\rangle} t_{ij} a_i^\dagger a_j. \quad (1)$$

The BHH provides an accurate description of cold-atom systems in which the optical lattice potential is strong enough that only the lowest Bloch band is significantly occupied [6]. In Eq. (1), $a_i^\dagger$ is the boson creation operator at site i, $n_i = a_i^\dagger a_i$ is the number operator, t_{ij} is the hopping amplitude between sites i and j, U is the on-site interaction energy, μ is the chemical potential, and ϵ_i is an energy offset due to the trap or to other intended or unintended local potentials. For a translationally invariant system with nearest-neighbor hopping, mean-field theory produces a phase diagram in μ/U-t/U space in which SF states are interrupted at small t/U by a series of MI lobes centered on half-odd integer values of μ/U, each characterized by a different fixed integer value N of the number of atoms per site (Fig. 1). Since t decreases and U increases with optical lattice potential strength, t/U can be experimentally varied over a wide range.

Depending on the regimes of the model's parameter space, different approximation schemes can be employed to study the BHH. For instance, in the small t/U limit atom number fluctuations on a given site due to hopping can be treated as weak perturbations. Even near the SF-MI transition strong interactions still suppress number fluctuations significantly, reducing the physically relevant Fock subspace to two or three number states and justifying mappings which transform the BHH into spin models that can be attacked using a large arsenal of extensively developed techniques [7]. On the other hand, for large values of t/U, the interactions between cold atoms are weak enough to justify Bogoliubov's weakly interacting boson theory. For large numbers of atoms per unit cell one can often employ the rotor approximation, $a_i \cong \sqrt{\bar{n}}e^{i\theta_i}$, that is valid when the mean occupation number $\bar{n}$ at each site is so large that its relative fluctuations are small. The resulting Hamiltonian is a quantum phase model in which the degrees of freedom are the phases of the superfluid at different sites. In this limit interactions induce phase fluctuations around a mean-field state in which all sites adopt a common phase [8]. All of these approaches have disadvantages in describing realistic optical lattice experimental systems which may have local superfluidity in one part of the system and local insulating behavior in another and which typically have a mean boson number on each lattice site of order 1 [9,10]. Our approach

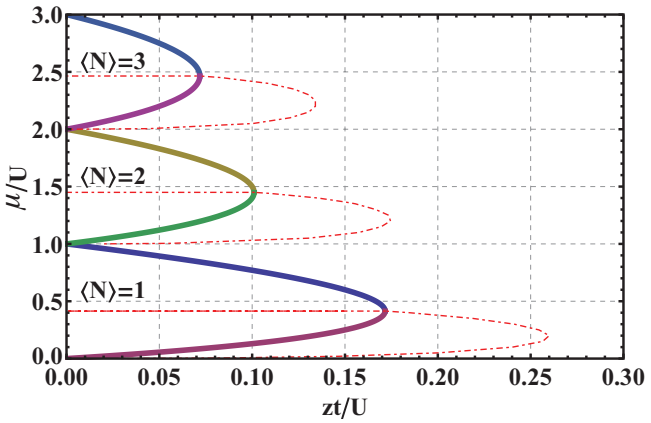

FIG. 1. (Color online) Mean-field phase diagram of the BHH. The solid lobes correspond to the MI phases, characterized by integer occupation of atomic sites. z is the coordination number, the number of neighbors of any given site. For sufficiently large values of zt/U, the system enters the SF phase. The dashed curves are contours along which the coherence field Berry curvature vanishes (see text).

has goals that are similar to those of other complementary approximate theories [11–27]. We seek an approach that can adequately describe the physics of the BHH in both insulating and superfluid regimes and is simple enough that it can be applied in the presence of inhomogeneities. One advantage of our approach is that we treat interactions exactly, a feature most useful in describing strongly correlated systems.

Our paper is organized as follows. In Sec. II, we describe the flexible formalism that is the subject of this paper. In practical applications it leads to a quadratic action for elementary excitations of uniform or nonuniform interacting bosons. In Sec. III, we report on illustrative applications first to the case of a uniform BHH with constant intersite tunneling amplitudes and then, as an example of a nonuniform system, to the case of a uniform BHH with fully frustrated intersite tunneling amplitudes. In Sec. IV we discuss the limitations of our theory before concluding with a brief summary.

II. FORMALISM

Our approach is based on single-site interacting boson wave functions $|\psi(\Sigma)\rangle$ which depend on a complex parameter Σ and are defined as Fock-space normalized ground states of the following single-site Hamiltonian,

$$h(\Sigma) = \frac{U}{2} n(n-1) - \mu n - \Sigma a^\dagger - \bar{\Sigma} a. \tag{2}$$

Note that the potential Σ induces coherence between single-site states with different boson occupation numbers. The mean-field theory of the BHH SF-MI phase transition [28] can be derived by considering variational wave functions of the following form,

$$|\Psi(\Sigma)\rangle_{\mathrm{MF}} = \prod_i |\psi_i\rangle. \tag{3}$$

These mean-field wave functions do not allow for correlated intersite fluctuations. The mean-field ground state is determined by minimizing

$$E(\Sigma) \equiv \frac{\langle\Psi(\Sigma)|H_{\mathrm{BHH}}|\Psi(\Sigma)\rangle}{\langle\Psi(\Sigma)|\Psi(\Sigma)\rangle} \tag{4}$$

with respect to the variational parameter Σ. In the SF state $\Sigma_{\mathrm{MF}} \neq 0$.

Our approach is to elevate Σ from a variational parameter to a quantum variable with correlated spatial fluctuations by allowing it to depend on site and on imaginary time [$\Sigma \to \Sigma_i(\tau)$] and then to construct an action S which depends on these fluctuations [29,30],

$$S = \int_0^\beta d\tau \left[\sum_i \langle\psi(\Sigma_i(\tau))|\partial_\tau \psi(\Sigma_i(\tau))\rangle_i + E[\Sigma] \right]. \tag{5}$$

Here at each instant of imaginary time

$$E[\Sigma] = \frac{\langle\Psi[\Sigma]|H_{\mathrm{BHH}}|\Psi[\Sigma]\rangle}{\langle\Psi[\Sigma]|\Psi[\Sigma]\rangle}, \tag{6}$$

and the correlated product state is given by

$$|\Psi[\Sigma]\rangle = \prod_i |\psi(\Sigma_i)\rangle_i. \tag{7}$$

In practice, the action can be evaluated analytically only if the coherence fields are expanded to leading order around their mean-field values. The main advantage of this approach, as stressed above, is its convenience in practical calculations, especially for nonuniform systems. Before we elaborate on this point, we examine some formal properties of our single-site interacting boson wave functions $|\psi(\Sigma)\rangle$.

A. Formal properties of the wave function $|\psi(\Sigma)\rangle$

One method of characterizing the Fock-space wave functions $|\psi(\Sigma)\rangle$ is to consider their expansion in terms of number eigenstates,

$$|\psi(\Sigma)\rangle = \sum_{n=0}^{\infty} c_n(|\Sigma|) \exp(in\phi_\Sigma)|n\rangle, \tag{8}$$

where we have noted that the magnitude of the expansion coefficients depends only on $|\Sigma|$ and defined ϕ_Σ as the phase of Σ. In Fig. 2 we plot $c_n^2 = |\langle n|\psi(\Sigma)\rangle|^2$ versus $|\Sigma|$ for a variety of n values for both $\mu/U = 0.4$, which falls inside the $N = 1$ MI lobe and for $\mu/U = 1.0$ at the boundary of the $N = 1$ and $N = 2$ MI lobes. This plot illustrates why spin model approximations to the BHH are justified close to the transition (for small values of $|\Sigma|$), since a small number of number states dominate. As one goes deeper into the SF region, the potential Σ induces coherence among more number states and spin-model approximations will fail.

The mean-field state is characterized by a time-independent field Σ_{MF} that minimizes the energy,

$$\left.\frac{\partial E}{\partial \Sigma_i}\right|_{\mathrm{MF}} = 0. \tag{9}$$

[The first term of Eq. (5) does not contribute to the action if Σ is time independent.] Quantum fluctuations are incorporated by employing a Gaussian-fluctuations approximation, $\Sigma_i = \Sigma_{\mathrm{MF}} + z_i$. Since the time dependence comes from the

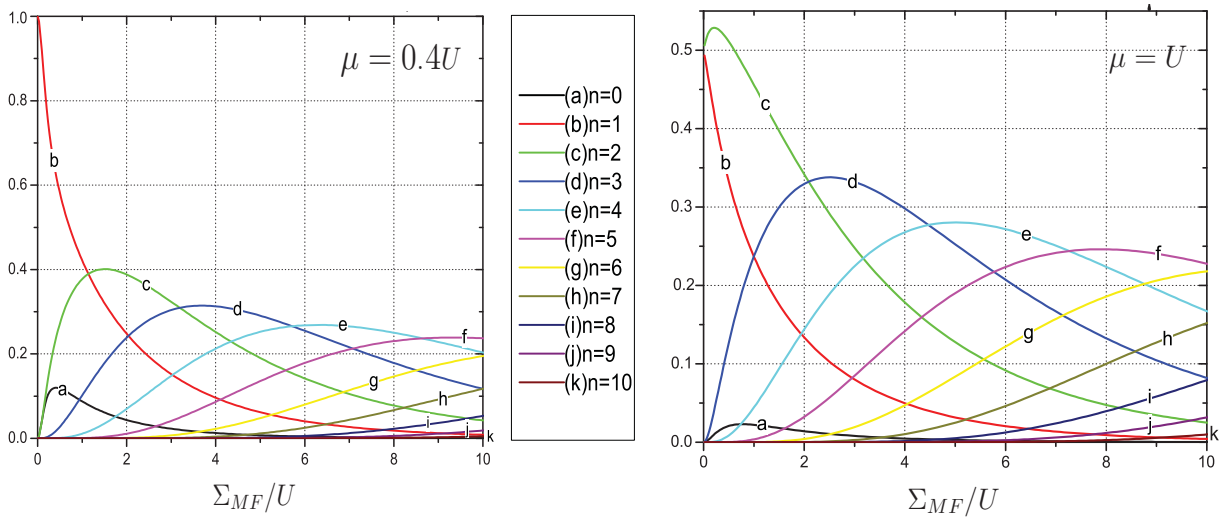

FIG. 2. (Color online) The overlap of our interacting wave functions with Fock number states, $|\langle n|\psi(\Sigma_{\rm MF})\rangle|^2$. Deep inside the SF phase (large $|\Sigma_{\rm MF}|$), more number states come into play, the result of strong atom number fluctuations. At $\mu = 0.4U$, only one Fock state, viz. $|n = 1\rangle$, is dominant close to the phase boundary (small $|\Sigma_{\rm MF}|$), whereas there are two, $|n = 1\rangle$ and $|n = 2\rangle$, at $\mu = U$, in accordance with Fig. 1.

fields only, we expand the time derivative in the Berry phase term as

$$\partial_\tau = \frac{\partial}{\partial \Sigma_i}\dot{\Sigma}_i + \frac{\partial}{\partial \bar{\Sigma}_i}\dot{\bar{\Sigma}}_i = \partial_{\Sigma_i}\dot{z}_i + \partial_{\bar{\Sigma}_i}\dot{\bar{z}}_i. \tag{10}$$

Substituting this in the action enables us to rewrite the first term of Eq. (5), the Berry phase term, as $\mathcal{C}_i(\Sigma_{\rm MF})\bar{z}_i\dot{z}_i$, where the gauge invariant Berry curvature of site i $\mathcal{C}_i$, evaluated at $\Sigma_{\rm MF}$, is given by [31]

$$\mathcal{C}_i(\Sigma_{\rm MF}) = \left\langle \frac{\partial\psi_i}{\partial\bar{\Sigma}_i}\middle|\frac{\partial\psi_i}{\partial\Sigma_i}\right\rangle - \left\langle \frac{\partial\psi_i}{\partial\Sigma_i}\middle|\frac{\partial\psi_i}{\partial\bar{\Sigma}_i}\right\rangle. \tag{11}$$

The Berry phase contribution to the action specifies the quantization condition of our fluctuating variables and plays an essential role in determining elementary excitation energies.

The energy functional, Eq. (6), can also be expanded around its mean-field value,

$$E[\Sigma] = E_{\rm MF} + \frac{1}{2}\sum_{ij}\left[\left.\frac{d^2E}{d\Sigma_i d\Sigma_j}\right|_{\rm MF} z_i z_j + \left.\frac{d^2E}{d\bar{\Sigma}_i d\Sigma_j}\right|_{\rm MF}\bar{z}_i z_j + \text{c.c.}\right], \tag{12}$$

where i and j stand for lattice sites and c.c. for complex conjugate. Combining the Berry phase term with the second-order contribution to the energy functional $E^{(2)}$, we construct a quadratic action from which we can use to calculate the elementary excitations. $S \cong S_{\rm MF} + S^{(2)}[\bar{z}_i, z_i]$, where

$$S^{(2)}[\bar{z}_i, z_i] = \int_0^\beta d\tau \sum_i \left[\mathcal{C}_i(\Sigma_{\rm MF})\bar{z}_i\dot{z}_i + E^{(2)}[\Sigma]\right]. \tag{13}$$

$E^{(2)}[\Sigma]$ contains all the second-order terms of (12).

B. Single site states at large *n*

Further insight into the properties of the single-site Hamiltonian, Eq. (2), can be obtained by examining the quantum phase model,

$$h(\Sigma) = \frac{U}{2}n(n-1) - \mu n - 2\sqrt{n}|\Sigma|\cos(\theta - \theta_\Sigma), \tag{14}$$

that is derived from Eq. (2) by letting $\Sigma \to |\Sigma|e^{i\theta_\Sigma}$, and employing the rotor approximation $a \to \sqrt{n}e^{i\theta}$, which is valid when number density fluctuations are small. In the rest of this section we write Σ for $|\Sigma|$. Assuming that quantum fluctuations are small allows us to determine the average atom number $n_o \sim (\Sigma/U)^{2/3}$ and phase $\theta_o = \theta_\Sigma$ by minimizing $h(\Sigma)$ with respect to n and θ. In addition, we can expand Eq. (14) to second order about the extrema n_o and θ_Σ to arrive at the quadratic Hamiltonian,

$$h(\Sigma) = \text{const} + \frac{3U}{4}(n - n_o)^2 + \frac{\Sigma^{4/3}}{U^{1/3}}(\theta - \theta_\Sigma)^2. \tag{15}$$

Phase and atom number are conjugate variables and we, therefore, recognize (15) as a quantum harmonic oscillator Hamiltonian. Using this analogy, we find the energy level spacing $\omega = \sqrt{3}U^{1/3}\Sigma^{2/3}$, mass $m = 2/3U$, typical density fluctuation $\delta n \equiv \langle(n - n_o)^2\rangle^{1/2} \sim (\Sigma/U)^{1/3}$, and typical phase fluctuation $\delta\theta \equiv \langle(\theta - \theta_\Sigma)^2\rangle^{1/2} \sim (U/\Sigma)^{1/3}$. We see that density fluctuations are suppressed and phase fluctuations enhanced as $\Sigma_{\rm MF}$ approaches 0 at the MI transition boundary.

The harmonic oscillator analog, based on the identifications $p \leftrightarrow \delta n$ and $q \leftrightarrow \delta\theta$, can also be used to derive an expression for the on-site Berry curvature that is valid at large Σ. The Berry curvature is determined by the dependence of the single-site wave function on the magnitude and phase of Σ. We, therefore, consider the influence of perturbations on the

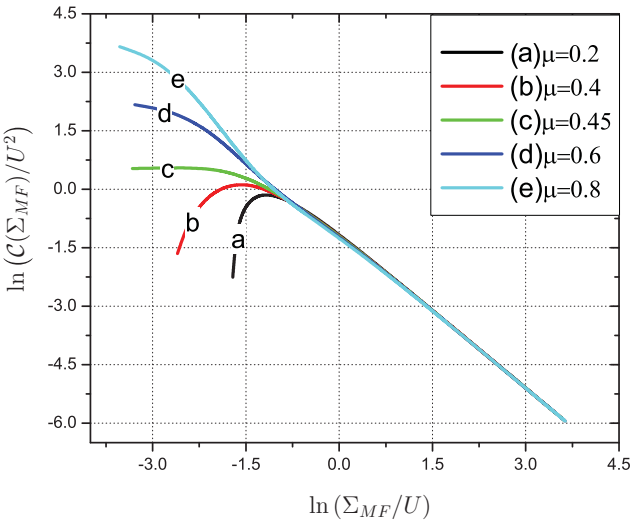

FIG. 3. (Color online) A log-log plot of the Berry curvature as a function of the coherence field $|\Sigma_{\rm MF}|$. Note the power-law decay rule $\mathcal{C}_i(\Sigma_{\rm MF}) \sim |\Sigma_{\rm MF}|^{-4/3}$ at large $|\Sigma_{\rm MF}|$ values predicted by Eq. (19). This plot is calculated from Eq. (11). The chemical potentials μ are measured in units of U.

eigenstates of Eq. (15),

$$h' = \frac{p^2}{2m} + \frac{1}{2}m\omega^2 q^2 - \lambda_p p - \lambda_q q = h - \lambda_p p - \lambda_q q. \tag{16}$$

To first order in λ_p and λ_q the ground state of h' is given by

$$|\phi_o\rangle' = |\phi_o\rangle + \sum_{n\neq o} \frac{\langle\phi_n|\lambda_p p + \lambda_q q|\phi_o\rangle}{\varepsilon_n - \varepsilon_o}|\phi_n\rangle. \tag{17}$$

where ε_n and $|\phi_n\rangle$ are the eigenvalues and eigenfunctions of h. It follows that the harmonic oscillator Berry curvature is given by [cf. Eq. (11)]

$$\begin{aligned}\mathcal{C} &= \mathrm{Im}\left[\left\langle\frac{\partial\phi}{\partial\lambda_2}\middle|\frac{\partial\phi}{\partial\lambda_1}\right\rangle - \left\langle\frac{\partial\phi}{\partial\lambda_1}\middle|\frac{\partial\phi}{\partial\lambda_2}\right\rangle\right] \\ &= \sum_{n\neq o}\mathrm{Im}\left[\frac{\langle\phi_o|p|\phi_n\rangle\langle\phi_n|q|\phi_o\rangle - \langle\phi_o|q|\phi_n\rangle\langle\phi_n|p|\phi_o\rangle}{(\varepsilon_n-\varepsilon_o)^2}\right].\end{aligned} \tag{18}$$

The matrix elements in this expression can be evaluated using $[h,p] = im\omega^2 q$ and $[h,q] = -ip/m$ to find

$$\mathcal{C}(\Sigma) = \frac{1}{\omega^2} \tag{19}$$

and hence for our single-site states $C \sim \Sigma^{-4/3}$ at large Σ. This result is confirmed by the plot (Fig. 3) of Berry curvature values numerically obtained from Eq. (11).

III. APPLICATION TO THE BOSE-HUBBARD HAMILTONIAN

We now test the theory's practical utility, first, by applying it to the BHH for a uniform optical lattice and, second, by applying it to the fully frustrated BHH which has four atoms per unit cell and, therefore, introduces inhomogeneity.

Separating Σ_i into its mean-field and fluctuation contributions, the single-site Hamiltonian h_i becomes

$$h_i = \frac{n_i(n_i-1)}{2} - \mu n_i - a_i^\dagger \Sigma_{\rm MF} - a_i \bar{\Sigma}_{\rm MF} - a_i^\dagger z_i - a_i \bar{z}_i. \tag{20}$$

The fluctuations are treated perturbatively. We write

$$|\psi\rangle_i = |\psi_o\rangle_i + |\psi_\Sigma\rangle_i z_i + |\psi_{\bar\Sigma}\rangle_i \bar{z}_i, \tag{21}$$

where

$$|\psi_\Sigma\rangle_i = \frac{\partial|\psi\rangle_i}{\partial\Sigma_i} = -\sum_{n\neq 0}\frac{{}_i\langle\psi_n|a_i^\dagger|\psi_o\rangle_i}{E_o - E_n}|\psi_n\rangle_i. \tag{22}$$

Here $|\psi_n\rangle_i$ and E_n are the eigenstates and the energy levels of the unperturbed on-site Hamiltonian. With Eq. (22), the Berry curvature can be calculated from Eq. (11) quite easily. The energy of the system, given by Eq. (6), can also be expanded (to quadratic order) in terms of the fluctuating fields [cf. Eq. (12)],

$$E = E^{(o)} + \sum_i E_{\Sigma_i} z_i + \sum_{ij}(E_{\Sigma_i\Sigma_j} z_i z_j + E_{\bar\Sigma_i\Sigma_j}\bar{z}_i z_j) + \text{H.c.}, \tag{23}$$

where we naturally identify

$$E_{\Sigma_i} = \left.\frac{\partial E}{\partial\Sigma_i}\right|_{\rm MF}, E_{\Sigma_i\Sigma_j} = \frac{1}{2}\left.\frac{\partial^2 E}{\partial\Sigma_i\partial\Sigma_j}\right|_{\rm MF}, \ldots. \tag{24}$$

The indices i and j refer to either same site or neighboring sites. For a uniform lattice, both the Berry curvature and the energy derivatives are independent of site indices. The mean-field state is determined by setting the first derivative terms to zero. The MI phase boundary is defined by the largest value of t/U for a given μ/U for which the energy is miminized by $|\Sigma| = 0$ on all sites. For the uniform BHH this procedure reproduces the familiar phase diagram plotted in Fig. 1.

A. Elementary excitations in a uniform lattice

To determine the elementary excitations of the BHH [15], we turn to the second-order action, Eq. (13), where we use Eq. (23) for the energy functional. For a uniform lattice, we Fourier-transform the fluctuations z_i,

$$z_i = \frac{1}{\beta\sqrt{N}}\sum_{k,n} z_{kn} e^{i(\mathbf{k}\cdot\mathbf{r}_i - \omega_n\tau)}, \tag{25}$$

where β is the inverse temperature, ω_n are the Matsubara frequencies, and N is the number of sites in the lattice. The resulting action is

$$\begin{aligned}S^{(2)}[\bar{z}z] &= \frac{1}{\beta}\sum_{k,n}[-i\omega_n\,\mathcal{C}(\Sigma_{\rm MF})\bar{z}_{kn}z_{kn} + \bar{z}_{kn}A_k z_{kn} \\ &\quad + z_{kn}\bar{B}_k z_{-k-n} + \bar{z}_{kn}B_k\bar{z}_{-k-n}] \\ &= \frac{1}{\beta}\sum_{k,n\geqslant 0}[\bar{z}_{kn}\ z_{-k-n}]\,M(\mathbf{k},n)\begin{bmatrix} z_{kn} \\ \bar{z}_{-k-n}\end{bmatrix},\end{aligned} \tag{26}$$

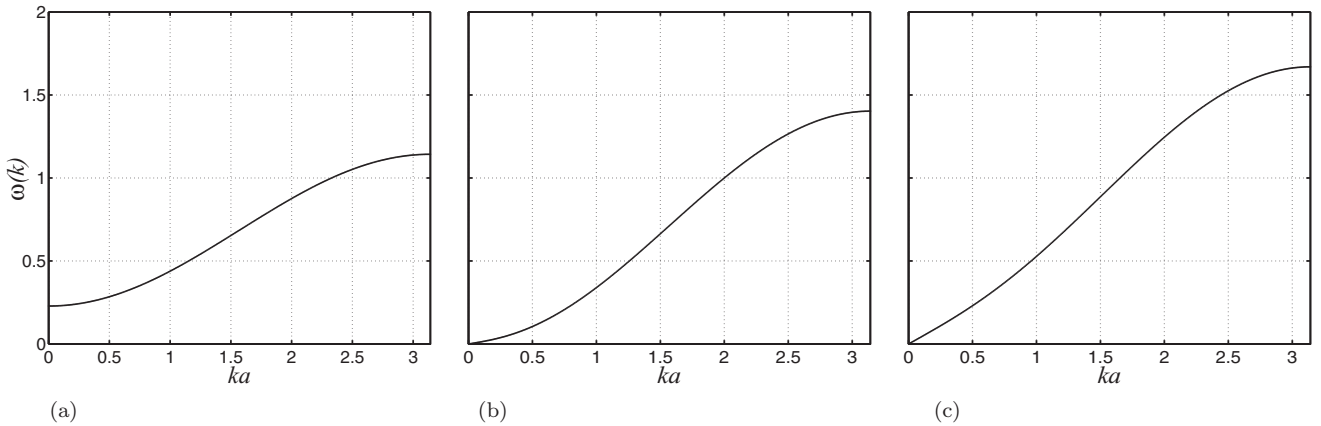

FIG. 4. (a) Dispersion inside the MI region. (b) Dispersion at the phase boundary. (c) Dispersion inside the SF phase. Elementary excitation energy $\omega(k)$ vs. k for a two dimensional uniform BHH along the line, $k \equiv k_x = k_y$ (a is the lattice constant). Note that the spectrum is gapped in the insulating phase and gapless at and beyond the phase boundary. Also note that for small $\mathbf{k}$, the dispersion is linear in the SF region, in accordance with Goldstone's theorem. In this approximate theory the dispersion is quadratic at the phase boundary. $\omega(k)$ is measured in units of U.

where

$$M(\mathbf{k},n) = \begin{bmatrix} -i\omega_n \mathcal{C}(\Sigma_{\rm MF}) + A_k & \bar{B}_k \\ B_k & i\omega_n \mathcal{C}(\Sigma_{\rm MF}) + A_k \end{bmatrix},$$
$$A_k = \frac{1}{2}\left.\frac{\partial^2 E}{\partial \bar{\Sigma}_i \partial \Sigma_i}\right|_{\rm MF} + \left.\frac{\partial^2 E}{\partial \bar{\Sigma}_i \partial \Sigma_j}\right|_{\rm MF} [\cos(k_x a) + \cos(k_y a)],$$
$$B_k = \left.\frac{\partial^2 E}{\partial \Sigma_i \partial \Sigma_i}\right|_{\rm MF} + \left.\frac{\partial^2 E}{\partial \Sigma_i \partial \Sigma_j}\right|_{\rm MF} [\cos(k_x a) + \cos(k_y a)], \tag{27}$$

and a is the lattice constant. Here, the indices i and j denote neighboring sites. By setting the determinant of the matrix $M(\mathbf{k},n)$ in Eq. (26) to zero, we obtain an expression for the excitation spectrum,

$$\omega(k) = \frac{\sqrt{A_k^2 - |B_k|^2}}{\mathcal{C}(\Sigma_{\rm MF})}. \tag{28}$$

In accordance with Goldstone's theorem, Eq. (28) yields a gapless Goldstone mode in the SF phase with linear dispersion at long wavelengths [Fig. 4(c)]. As the MI phase boundary is approached and crossed, excitations become more localized and the mode dispersion weakens [Fig. 4(b)] and [Fig. 4(a)]. At certain points in the phase diagram the Berry curvature $\mathcal{C}(\Sigma_{\rm MF})$ vanishes (Fig. 1) and our theory of the excitation spectrum becomes unreliable. We return to this point in the discussion section.

B. Fully frustrated lattices

As mentioned above, the theory outlined in Sec. II is designed with inhomogeneous systems in mind and is general enough to be applied to systems where the translational symmetry is reduced, or altogether lost. We demonstrate this with the case of a two-dimensional uniform lattice in which the tunneling amplitude sign alternates in one direction (see Fig. 5). This hopping model corresponds to a half-flux quantum per square lattice plaquette and is referred to as a fully frustrated BHH [32]. For this case we allow translational symmetry to be broken by doing the mean-field minimization for a lattice with four sites per unit cell. The quadratic theory is similarly modified, with the M matrix in Eq. (27) enlarging to an eight by eight matrix.

A detailed mean-field study of the quantum phase transitions in the fully frustrated lattice has been carried out elsewhere [33]. Here we apply Eq. (9) on each site of a plaquette to find the mean-field values of the fields, $\Sigma_A, \Sigma_B, \Sigma_C$, and Σ_D. The elementary excitations of the system follow from the second order action, Eq. (13). We take advantage of the (reduced) translational symmetry by Fourier decomposing the fluctuation fields at each site,

$$z_{sl}(\mathbf{r},\tau) = \frac{1}{\beta\sqrt{N}} \sum_k z_{sk}(\tau) e^{i\mathbf{k}\cdot\mathbf{r}_l}, \tag{29}$$

where l refers to plaquettes and s to the four sites (A, B, C, and D) within a given plaquette. The Berry phase term,

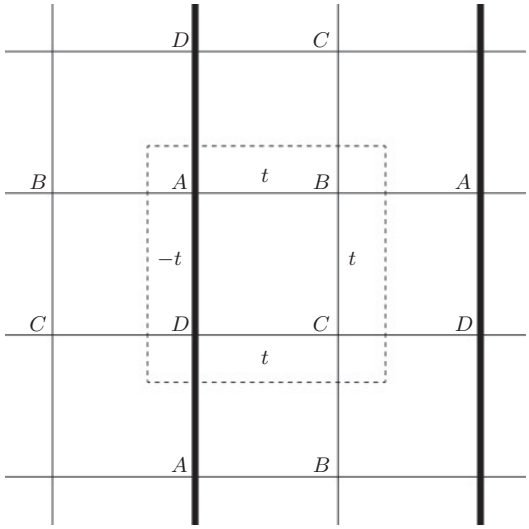

FIG. 5. Fully frustrated lattice. The thick bonds are the links with hopping amplitude $t_{ij} = -t$ that frustrate intersite coherence. The dashed box contains a unit cell of the frustrated lattice.

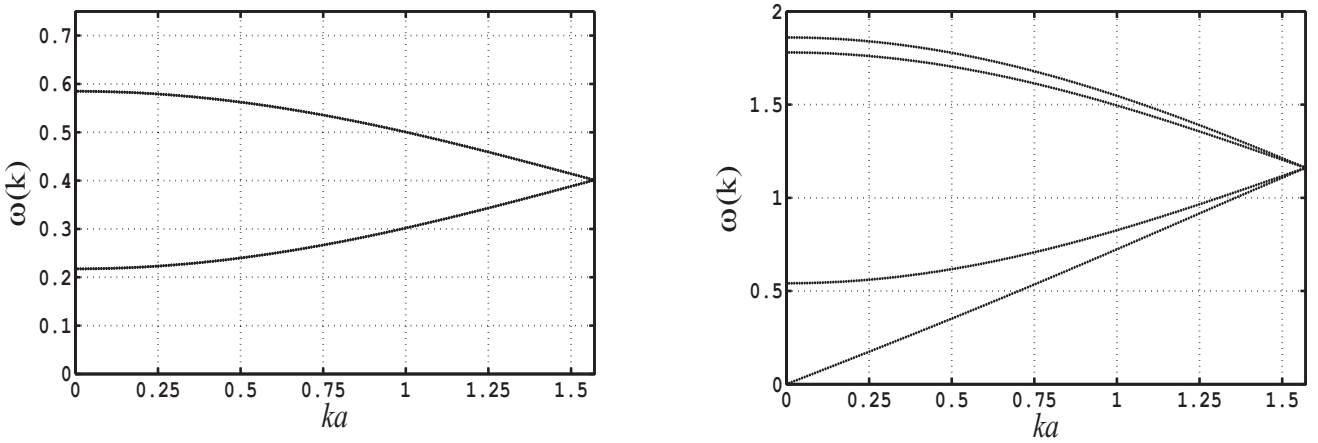

FIG. 6. (a) Excitation modes inside the MI phase. Each mode is doubly degenerate. (b) Excitation modes inside the SF phase. Elementary excitations of the fully frustrated lattice plotted along $k \equiv k_x = k_y$ (a is the lattice constant). The lowest dispersion is gapped inside the insulator and gapless beyond the phase boundary. Again, obeying Goldstone's theorem, the lowest dispersion in the SF phase is gapless and linear at small k; $\omega(k)$ is measured in units of U.

calculated at the mean-field state defined by the above four fields, becomes

$$\sum_{sk} \mathcal{C}_s \bar{z}_{sk}(\tau)\partial_\tau z_{sk}(\tau), \tag{30}$$

while the energy term contains all the second-order deviations of the energy about this mean-field state. Replacing $z_{sk}(\tau) \to \sqrt{\mathcal{C}_s} z_{sk}(\tau)$ reduces the action into the standard form

$$S^{(2)} = \int_0^\beta d\tau \sum_{k,s} \{\bar{z}_{sk}(\tau)\partial_\tau z_{sk}(\tau) + E^{(2)}[\bar{z}_{sk}(\tau), z_{sk}(\tau)]\}. \tag{31}$$

Having elevated the fluctuations into quantum variables (obeying bosonic commutation relations), we are now in a position to employ the transformation $\vec{z} = \mathcal{B}\vec{v}$, where $\vec{z} = [\begin{smallmatrix} z_{sk}(\tau) \\ \bar{z}_{s-k}(\tau) \end{smallmatrix}]$, that preserves the commutation relations and perform Bogoluibov diagonalization [34,35] to transform the action into

$$S^{(2)} = \int_0^\beta d\tau \sum_k [\bar{v}_k \partial_\tau v_k + \omega(k)\bar{v}_k v_k], \tag{32}$$

from which we can easily identify $\omega(k)$ as the excitation spectrum. A few sample plots of the dispersion are shown in Fig. 6.

We now sketch out the extension of this approach to the case of lattices with even less symmetry (optical lattices in harmonic traps, for example) or to entirely inhomogenous ones (disordered lattices). For a lattice with N sites, the mean-field state is determined by solving the N coupled equations, Eq. (9), for the coherence fields $\Sigma_{i,\mathrm{MF}}$. Vanishing or finite values of $\Sigma_{i,\mathrm{MF}}$ determine the absence or presence of superfluid order on a given site i, respectively. In solving the coupled equations, it is, of course, advisable to take advantage of the reduced symmetry, if present, as we have done here with the fully frustrated lattice (for a lattice in an isotropic harmonic trap, one can appeal to rotational symmetry to significantly reduce the degrees of freedom). Once $\Sigma_{i,\mathrm{MF}}$ are obtained, the second-order terms that go into the action, Eq. (13) can be read off from Eqs. (23) and (24). The extraction of the excitation energies from the action [34,35], similar to the steps that led to Eq. (32) is described in the appendix. In this manner, one can determine the basic properties, i.e., the ground state as well as the low-energy excitations of interacting bosonic systems in a lattice in the presence of spatial inhomogeneities.

IV. DISCUSSION

As demonstrated above, the Berry phase is the critical ingredient in formulating the quantum theory and calculating the elementary excitations from it. As such, the excitation spectra one obtains become unreliable if and when the Berry curvature vanishes. The dashed curves in Fig. 1 trace the contours in the phase diagram where the Berry curvature, Eq. (11), of the uniform BHH becomes zero. One point of view toward restoring the quantum theory is to retain terms that are second order in time derivative in deriving the action, Eq. (5) [36,37]. Here, we content ourselves to exploring the consequences of a vanishing Berry curvature to our theory. To have a better understanding of these special points, we focus on the MI phases, where the Berry curvature is explicitly given by

$$\mathcal{C} = \frac{n+1}{\left(\frac{\mu}{U} - n\right)^2} - \frac{n}{\left(n - 1 - \frac{\mu}{U}\right)^2}. \tag{33}$$

For $n = 1$, for instance, $\mathcal{C}$ vanishes at $\mu/U = \sqrt{2} - 1$, corresponding to a set of points in the phase diagram with particle-hole symmetry. In other words, in our formalism, there is no distinction between the definitions for the annihilation and creation operators that emerge from quantizing the fluctuations, rendering their commutator zero. This is consistent with the results of Ref. [5], where quantum phase transitions at the tips of the MI phases, the multicritical points with particle-hole

symmetry, belong to the universality class of the XY model, where the time derivative is second order, in contrast to anywhere else across the phase boundary where it is first order, and there is an absence of particle-hole symmetry [5,8].

In summary, the relative ease with which the above theory has determined the basic properties of the fully frustrated optical lattice higlights its main focus: inhomogenous systems, such as optical lattices in symmetry breaking harmonic traps, or experimental set-ups with controlled disorder, which have generated lots of interest lately [38]. Our theory complements previous efforts that have studied the BHH, and its results, such as the mean-field phase diagram and the excitation modes compare well with past conclusions [11–27]. The advantage of our formalism is its broad applicability to systems that are not spatially uniform, as is the case with most *real-world* experimental setups. In addition, for these setups, the simplicity, and accuracy of our theory make it a relatively convenient mechanism to interpret the experimental results. Though we have focused here at zero temperature, we do not anticipate any particular difficulty in extending the theory to finite temperatures. It may also be interesting to modify the theory developed here for other lattice Hamiltonians, such as those involving next-neighbor interactions, where interesting phases such as charge density waves and supersolids are predicted [39].

ACKNOWLEDGMENTS

This work is supported by Welch Foundation under Grant No. F1473 and by DOE under Grant No. DE-FG03-02ER45985.

APPENDIX

In this section, we discuss some of the diagonalization procedure we employed above to arrive at Eq. (32). The need to perform Bogoliubov diagonalization of many degrees of freedom arises in most considerations of many-body problems, especially inhomogenous ones, and there are now a number of sources in the literature one can consult for more details [34,35]. Here we give a more succint summary. Let

$$\vec{z} = \begin{bmatrix} z_i \\ \bar{z}_i \end{bmatrix} = \begin{bmatrix} z_1 \\ z_2 \\ \vdots \\ z_N \\ \bar{z}_1 \\ \bar{z}_2 \\ \vdots \\ \bar{z}_N \end{bmatrix},$$

where N is the total number of sites in the optical lattice. As mentioned above, these fluctuations are now quantum variables, and thus obey bosonic commutation relations, $[\vec{z},\vec{z}^\dagger] = \mathcal{I}$, where $\mathcal{I} = \begin{bmatrix} \mathbb{1} & 0 \\ 0 & -\mathbb{1} \end{bmatrix}$, with $\mathbb{1}$ and 0 being the $N \times N$ identity and zero matrices, respectively.

We introduce the Hamiltonian $\mathcal{H}$ such that second-order energy terms of the action, such as the one in Eq. (31), can be written as $E^{(2)}[\bar{z}_i, z_i] = \vec{z}^\dagger \mathcal{H} \vec{z}$. Our goal is to perform a canonical transformation $\vec{z} = \mathcal{B}\vec{v}$ that diagonalizes the Hamiltonian $\mathcal{H}$ while preserving the bosonic commutation relations,

$$\begin{aligned} \mathcal{B}^\dagger \mathcal{H} \mathcal{B} &= \mathcal{D} \\ [\vec{v},\vec{v}^\dagger] &= \mathcal{I}, \end{aligned} \tag{A1}$$

where $\mathcal{D} = \{\epsilon_1, \epsilon_2, \ldots, \epsilon_{2N}\}$ are the eigenmodes of interest. Using Eq. (A1) alongside the identities $\mathcal{B}^\dagger \mathcal{I} \mathcal{B} = \mathcal{I}$ (which follows from the commutation relations) and $\mathcal{I} = \mathcal{I}^{-1}$, we obtain the expression

$$\tilde{\mathcal{H}} \mathcal{B} = \tilde{\mathcal{D}} \mathcal{B}, \tag{A2}$$

where

$$\tilde{\mathcal{D}} \equiv \mathcal{I}^{-1}\mathcal{D} = \{\epsilon_1, \epsilon_2, \ldots, \epsilon_N, -\epsilon_{N+1}, -\epsilon_{N+2}, \ldots, -\epsilon_{2N}\}.$$

If we consider each vector $\vec{b}_i$ comprising the matrix $\mathcal{B}$, we see that Eq. (A2) is essentially an eigenvalue problem, where the eigenvalues are particle-hole pairs ($\epsilon_i = -\epsilon_{i+N}$), and ϵ_i, where $1 \leqslant i \leqslant N$ are the fundamental excitation modes of the theory such as those plotted in Fig. 6.

[1] M. Greiner, O. Mandel, T. Esslinger, T. W. Hansch, and I. Bloch, Nature **415**, 39 (2002).
[2] I. Bloch, J. Dalibard, and W. Zwerger, Rev. Mod. Phys. **80**, 885 (2008).
[3] L. Fallani, J. E. Lye, V. Guarrera, C. Fort, and M. Inguscio, Phys. Rev. Lett. **98**, 130404 (2007).
[4] M. Pasienski, D. McKay, M. White, and B. DeMarco, Nat. Phys. **6**, 677 (2010).
[5] M. P. A. Fisher, P. B. Weichman, G. Grinstein, and D. S. Fisher, Phys. Rev. B **40**, 546 (1989).
[6] D. Jaksch, C. Bruder, J. I. Cirac, C. W. Gardiner, and P. Zoller, Phys. Rev. Lett. **81**, 3108 (1998).
[7] A. Auerbach, *Interacting Electrons and Quantum Magnetism* (Springer, New York, 1994).
[8] S. Sachdev, *Quantum Phase Transitions* (Cambridge University Press, Cambridge, UK, 2000).
[9] S. Fölling, A. Widera, T. Müller, F. Gerbier, and I. Bloch, Phys. Rev. Lett. **97**, 060403 (2006).
[10] G. K. Campbell, J. Mun, M. Boyd, P. Medley, A. E. Leanhardt, L. G. Marcassa, D. E. Pritchard, and W. Ketterle, Science **313**, 649 (2006).
[11] D. S. Rokhsar and B. G. Kotliar, Phys. Rev. B **44**, 10328 (1991).
[12] W. Krauth, M. Caffarel, and J.-P. Bouchaud, Phys. Rev. B **45**, 3137 (1992).
[13] J. K. Freericks and H. Monien, Phys. Rev. B **53**, 2691 (1996).
[14] N. Elstner and H. Monien, Phys. Rev. B **59**, 12184 (1999).
[15] D. van Oosten, P. van der Straten, and H. T. C. Stoof, Phys. Rev. A **63**, 053601 (2001).

[16] D. B. M. Dickerscheid, D. van Oosten, P. J. H. Denteneer, and H. T. C. Stoof, Phys. Rev. A **68**, 043623 (2003).
[17] C. Schroll, F. Marquardt, and C. Bruder, Phys. Rev. A **70**, 053609 (2004).
[18] J. J. García-Ripoll, J. Cirac, P. Zoller, C. Kollath, U. Schollwöck, and J. von Delft, Opt. Express **12**, 42 (2004).
[19] K. Sengupta and N. Dupuis, Phys. Rev. A **71**, 033629 (2005).
[20] S. Konabe, T. Nikuni, and M. Nakamura, Phys. Rev. A **73**, 033621 (2006).
[21] B. Damski and J. Zakrzewski, Phys. Rev. A **74**, 043609 (2006).
[22] O. Fialko, C. Moseley, and K. Ziegler, Phys. Rev. A **75**, 053616 (2007).
[23] F. E. A. dos Santos and A. Pelster, Phys. Rev. A **79**, 013614 (2009).
[24] I. Danshita and P. Naidon, Phys. Rev. A **79**, 043601 (2009).
[25] T. P. Polak and T. K. Kopeć, Phys. Rev. B **76**, 094503 (2007).
[26] K. Byczuk and D. Vollhardt, Phys. Rev. B **77**, 235106 (2008).
[27] S. D. Huber, B. Theiler, E. Altman, and G. Blatter, Phys. Rev. Lett. **100**, 050404 (2008).
[28] K. Sheshadri, H. R. Krishnamurthy, R. Pandit, and T. V. Ramakrishnan, Europhys. Lett. **22**, 257 (1993).
[29] J. W. Negele and H. Orland, *Quantum Many-Particle Systems* (Perseus Books, New York, 1988).
[30] R. Jackiw and A. Kerman, Phys. Lett. A **71**, 158 (1979).
[31] M. V. Berry, Proc. R. Soc. London A **392**, 45 (1984).
[32] M. Polini, R. Fazio, A. H. MacDonald, and M. P. Tosi, Phys. Rev. Lett. **95**, 010401 (2005).
[33] D. Tilahun, Ph.D. dissertation, The University of Texas at Austin, 2008.
[34] U. Zulicke, Ph.D. dissertation, Indiana University, 1988.
[35] J.-P. Blaizot and G. Ripka, *Quantum Theory of Finite Systems* (The MIT Press, Cambridge, MA, 1985).
[36] J. R. Klauder, Phys. Rev. D **19**, 2349 (1979).
[37] R. Shankar, *Principles of Quantum Mechanics* (Springer, New York, 1994).
[38] L. Sanchez-Palencia and M. Lewenstein, Nat. Phys. **6**, 87 (2010).
[39] A. van Otterlo, K.-H. Wagenblast, R. Baltin, C. Bruder, R. Fazio, and G. Schön, Phys. Rev. B **52**, 16176 (1995).